Trees (2004) 18: 493–500
DOI 10.1007/s00468-004-0322-2

ORIGINAL ARTICLE

Eric M. Kramer · Michael H. Borkowski

Wood grain patterns at branch junctions: modeling and implications

Received: 18 August 2003 / Accepted: 23 January 2004 / Published online: 30 July 2004

Abstract We apply a recent model of wood grain pattern formation to the junction between two tree branches. In model simulations, the export of indole-3-acetic acid (IAA) from a branch into the junction is necessary to maintain the continuity between the grain pattern of the branch and the grain of the subjacent stem. Increased IAA export corresponds to a larger effect on the overall grain pattern. Conversely, if IAA export stops, the grain pattern diverts around the branch. These results do not depend on specific values for the model parameters and appear to be quite general. Since long-range water transport is largely parallel to the wood grain, greater IAA export from a branch is expected to give improved access to the water resources of the tree. IAA export thus emerges as a likely regulator of branch vigor. In this way, the basipetal flux of IAA through a branch, and its morphological consequences at branch junctions, may play an important role in several aspects of tree form.

Keywords Auxin · Wood grain · Pattern formation · Hydraulic architecture · Branch autonomy

Introduction

Branch junctions in trees are a subject of study for several reasons. Arboriculture is interested in the role branch junctions play in compartmentalizing wounds and protecting the tree from invading pathogens (Shigo 1985, 1991; Mattheck and Kubler 1995; Eisner et al. 2002a). Forest product engineers are interested in the consequences of branch junctions for the strength and durability of lumber sawn from the tree (Phillips et al. 1981; Green et al. 1999; Foley 2001). Tree physiologists and ecologists focus on the role junctions play in the hydraulic architecture of the tree (Tyree and Ewers 1991; Tyree and Alexander 1993; Aloni et al. 1997; Brooks et al. 2002; Eisner et al. 2002b). The pattern of wood grain at a branch junction has consequences for all these topics (Shigo 1985; Lev-Yadun and Aloni 1990; Andre 2000; Schulte and Brooks 2003).

Figure 1 shows the wood grain pattern at three branch junctions of white pine (*Pinus strobus*). The bark has been removed and the images have been processed to emphasize the striations that show grain direction. Note that live branches have grain that is continuous with the subjacent branch. By comparison, the grain diverts around the dead branch. The fact that live branches participate in the grain of the tree while dead branches are excluded has not received much comment from modern biologists. Conversely, the phenomenon is frequently discussed in the publications of forest product engineers, since grain patterns are critical to the properties of sawn lumber (Phillips et al. 1981; Green et al. 1999; Foley 2001).

The diversion of grain around a dead branch constitutes a regulatory mechanism that is vital to the continued survival of the tree. The grain direction is the primary direction of water transport through the xylem in both hardwoods and softwoods (Rudinsky and Vite 1959; Kozlowski and Winget 1963; Zimmermann and Brown 1971; Shigo 1985; Schulte and Brooks 2003). Thus, wood with grain that leads to a dead branch cannot efficiently supply water to live portions of the tree. In addition, the diversion of grain around a dead branch helps to strengthen the wood against cracks that might be initiated at that location (Mattheck and Kubler 1995).

There is a less obvious consequence of grain patterning, shown schematically in Fig. 2. The figure shows the grain of two similar branch junctions, differing only in the amount of grain the lateral branch "captures" from the subjacent stem. To the extent that water flow transverse to the grain is limited by high hydraulic resistance, branches that meet at a junction are effectively drawing water from distinct pathways in the stem (Brooks et al. 2002; Schulte and Brooks 2003). Thus, a lateral branch that captures a larger portion of the grain is expected to have improved

E. M. Kramer (✉) · M. H. Borkowski
Department of Physics, Simon's Rock College,
84 Alford Road,
Great Barrington, MA, 01230, USA
e-mail: ekramer@simons-rock.edu
Tel.: +1-413-5287476
Fax: +1-413-5287365

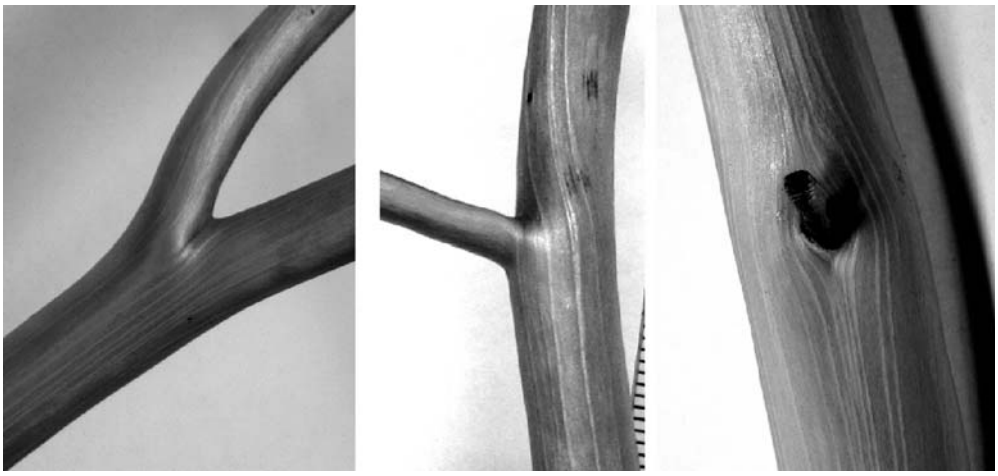

Fig. 1 Three digital images of junctions in debarked branches of white pine (*Pinus strobus*). The images have been processed to emphasize the path of resin canals which track the wood grain of the branch. From left to right, the branch diameters are 14, 9, and 14 mm

access to the water resources of the tree. Under water-limited growth conditions, the lateral branch that captures more grain will be more vigorous [for discussions of hydraulic limitation in the whole-tree context, see Ryan and Yoder (1997), Becker et al. (2000), and Sperry et al. (2002)]. Similarly, when two branches meet at a junction, their relative vigor may depend in part on the fraction of the grain each captures. Since there is only a finite circumference available in the subjacent branch, this represents a competition between branches.

It is helpful to review some of the standard vocabulary related to branch vigor. Discussions of branch vigor usually begin with the concepts of apical dominance and apical control (Brown et al. 1967; Zimmermann and Brown 1971; Cline 1997). Apical dominance is the suppression of the outgrowth of lateral buds by a vigorous distal branch. Apical control is the slowing of the elongation of lateral branches by a vigorous distal branch. Brown et al. (1967) cite the conical shape of a pine tree as typical of species with strong apical control. The vigorously growing topmost branch somehow slows the elongation of the lateral branches below it. Since our model is only appropriate to branches undergoing secondary growth (and not to buds), it is not applicable to discussions of apical dominance but may provide insights into apical control.

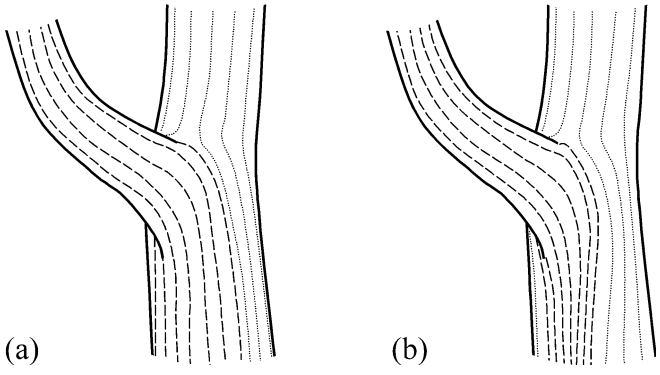

Fig. 2 Sketch of the wood grain at a hypothetical branch junction. *Dashed* grain lines lead to the branch on the left. The leftmost branch in **a** captures more of the grain from the subjacent stem than the leftmost branch in **b**. Under water-limited growth conditions, the leftmost branch in **a** will be more vigorous than the leftmost branch in **b**

The next concept is branch autonomy (Sprugel et al. 1991; Sprugel 2002). Branch autonomy is an approximation common in ecological modeling. It says that the vigor of a branch depends on its morphology and light environment but is otherwise independent of the tree to which it is attached. Sprugel (2002) describes several caveats to the concept of branch autonomy and emphasizes that the approximation is frequently false. In particular, the vigor of a lateral branch seems to depend on the vigor of the tree to which it is attached. He cites several examples of an inverse relationship—lateral branches on a stressed tree are more vigorous than similar lateral branches on an unstressed tree (Stoll and Schmid 1998; Takenaka 2000; Henriksson 2001). Sprugel calls this observation "Milton's Law." Milton's Law is superficially paradoxical, but it may be regarded as another manifestation of apical control. A vigorous tree crown is more effective at suppressing the growth of laterals than a shaded or otherwise stressed crown.

The assumption of branch autonomy may also fail when comparing similar branches within the same tree. Nikinmaa and coworkers have found that an accurate statistical description of tree crowns in Scots pine (*Pinus sylvestris*), sugar maple (*Acer saccharum*), and yellow birch (*Betula alleghaniensis*) requires the introduction of a branch position-dependent "vigor index" (Goulet et al. 2000; Nikinmaa et al. 2003). They state that "a lower branch grows less than an upper branch given similar size and light conditions" (Nikinmaa et al. 2003).

The regulation of wood grain pattern takes place in the vascular cambium, the relatively soft tissue that produces new wood [for reviews see Catesson (1990), Iqbal and Ghouse (1990), Larson (1994), and Savidge (1996)]. The cambium is usually <1 mm thick in the radial direction and forms a continuous cylindrical sheath around the wood of the branch. As the cambium moves gradually outward, it leaves behind daughter cells that differentiate into all the components of wood (called xylem elements). The grain pattern in the newly formed wood reiterates the orientation

ERRATUM

Eric M. Kramer and Michael H. Borkowski
"Wood grain patterns..."

Figure 3 **panel (b) corrected**

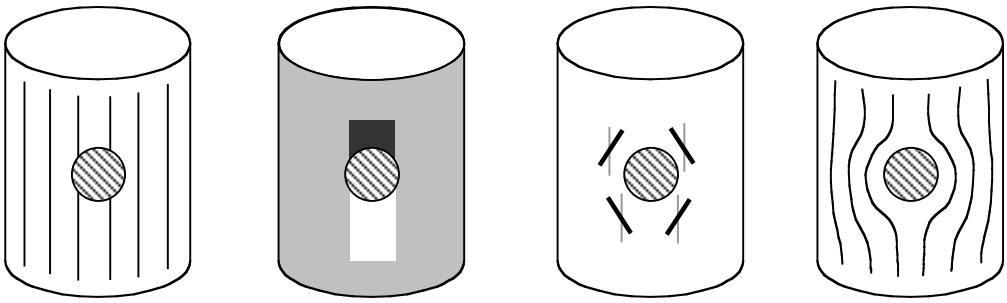

Equation (2) in Appendix 1 should read:

$$\nabla^2\mathbf{u} + \frac{2}{L^2}\mathbf{u}(1-u^2) + \frac{1}{\lambda}\left\{-(\nabla m)\left(\frac{3-u^2}{2}\right) + (\mathbf{u}\cdot\nabla m)\mathbf{u}\right\} = 0$$

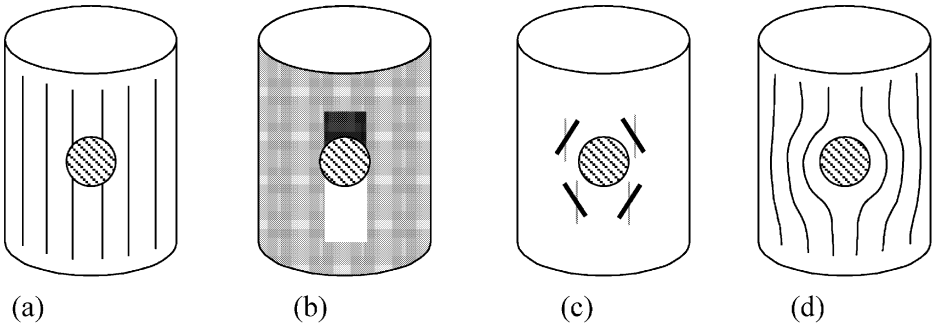

Fig. 3 Sketch of the stages in cambial re-orientation according to the model. **a** A circular wound (*hatched circle*) occurs in a cambial cylinder with initially straight grain. **b** Due to basipetal active transport, IAA accumulates above the wound and is depleted below (*grayscale* represents IAA concentration). **c** Fusiform initial cells (*solid lines*) gradually rotate so their apical tips point towards the local maximum of IAA concentration. **d** Newly formed wood grain circumvents the wound

of elongated fusiform initial cells in the cambium (Larson 1994). Since the orientation of mature xylem elements is unchangeable, wood grain pattern is established in the cambium through the coordinated orientation of the relatively plastic fusiform initials.

The preceding remarks suggest that live branches produce a signal that can influence the orientation of fusiform initials in the vascular cambium of the subjacent branch. A likely candidate for this signal is the ubiquitous auxin indole-3-acetic acid (IAA). IAA is synthesized mainly in growing buds and leaves and subsequently transported basipetally through the branches towards the roots [see (Kramer 2002) and citations therein. For a recent study of IAA synthesis in leaves, see (Aloni et al. 2003)]. In stems and branches, IAA is localized to the cambium and its adjacent derivatives (Uggla et al. 1996; Tuominen et al. 1997; Uggla et al. 1998), where it has been proposed to play a role in nearly every aspect of secondary growth. Two notable examples: (1) Aloni and Zimmermann (1983) proposed that the concentration of IAA in the cambium controls the radius and number density of newly-formed vessels in trees, and (2) Sundberg and coworkers (2000) suggested that the radial concentration gradient of IAA provides positional information that helps guide the development of differentiating xylem and phloem elements. Of particular relevance here are proposals that the flux of IAA determines the orientation of differentiating vascular tissues (Harris 1969; Kirschner et al. 1971; Zagorska-Marek and Little 1986; Harris 1989), since these provided the early basis for our model of wood grain pattern formation. Considered together, it seems unlikely that IAA alone could control all these aspects of vascular differentiation. Rather, as noted by Sundberg et al. (Sundberg et al. 2000), IAA probably plays a part in conjunction with other signals in the tree.

In this paper we apply a recent model of auxin-mediated wood grain pattern formation to a consideration of branch junctions (Kramer 2002; Kramer and Groves 2003). The model includes a simultaneous description of the IAA distribution in the cambium, the grain pattern in the cambium, and their interrelationship. The main qualitative features of the model are illustrated schematically in Fig. 3, and are discussed further in Materials and methods. Note that Kramer (2002) includes an early attempt at modeling a branch junction. In this paper we repeat the approach for a wide range of parameter values and a more realistic geometry.

The most interesting result reported here is that the amount of grain captured by a branch increases in proportion to the flux of indoleacetic acid (IAA) exported by the branch into the junction. This holds true for any reasonable choice of model parameters and thus seems to be quite general. We therefore suggest that IAA is the signal produced by a live branch that ensures its participation in the grain of the stem. When the branch dies, IAA export stops and the cambial grain reorients to avoid the branch.

Materials and methods

In this section we describe the basic features of the model presented in Kramer (2002) and Kramer and Groves (2003). Interested readers are referred to the previous references for a derivation of the model and details of the numerical methods. Some mathematical specifics of the model are discussed in Appendices 1 and 2.

The model approximates the cambium of a branch as a surface with negligible thickness in the radial direction. Model quantities are required to be sums or averages through the radial thickness of the cambium. The concentration of IAA is thus expressed as a mass per unit cambial area. This quantity has been measured in stems of Japanese cedar (*Cryptomeria japonica*), hybrid aspen (*Populus tremula*×*P. tremuloides*), red pine (*Pinus densiflora*), and Scots pine (*Pinus sylvestris*) (Funada et al. 1990; Sundberg et al. 1993; Tuominen et al. 1997; Uggla et al. 1998; Sundberg et al. 2000; Tuominen et al. 2000; Funada et al. 2001; Funada et al. 2002). Values for hybrid aspen fall in the range 10–40 (ng IAA)/cm^2, while typical values for the softwoods are about five times larger, 50–200 (ng IAA)/cm^2.

The model incorporates five points (see Fig. 3): (1) IAA undergoes active transport through the cambial region with speed v in a direction parallel to the grain. (2) The flux of IAA also has a diffusive contribution, with effective diffusion coefficients $D_{\parallel}$ and $D_{\perp}$ parallel and perpendicular to the grain, respectively. (3) Fusiform initials re-orient in response to transverse gradients in the distribution of IAA. The net effect of this response is that the grain tends to rotate until it points away from regions with locally high concentrations of IAA. The model parameter μ characterizes the strength of this effect. (4) Fusiform initials tend to align parallel to their neighbors due to interactions between cells. The model parameter K characterizes the strength of this interaction. (5) The

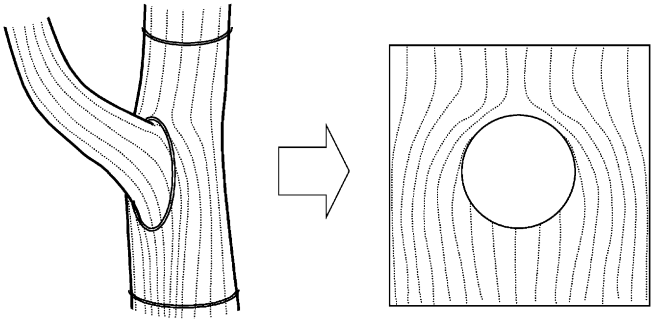

Fig. 4 Sketch illustrating the use of a square simulation domain to represent a portion of the cambium at a branch junction

synthesis and metabolization of IAA in the cambium is small compared to the net flux of IAA through the region under consideration.

Modeling a complex curved cambial surface is beyond the scope of the current paper, so we simplify the simulation domain as shown in Fig. 4. The domain is a flat square with a disk excised from the center. For definiteness we will refer to the straighter of the two branches as the main branch. The branch that joins at the disk is called the lateral branch. The figure makes clear that the simulation domain may be regarded as part of the cylindrical surface of the main branch. All simulations described in Results are for a square domain 34 mm on a side with an excised disk 3.0 mm in radius. We verified that simulations using other choices for the domain or branch size show the same qualitative features as those described in Results.

It will be helpful to define the net flux Φ of IAA through the cambial region of a branch. The net flux is the mass of IAA passing per unit time through a circumference of the branch. For a hypothetical branch 3.0 mm in radius, with 20 ng/cm^2 of IAA in the cambium and an active transport speed of 10 mm/h, the flux is $\Phi=2\pi(0.3\text{ cm})(20\text{ ng/cm}^2)(1.0\text{ cm/h})=38$ ng/h. It is also instructive to consider the mass of IAA per unit stem length. For our hypothetical branch we have $2\pi(0.3\text{ cm})(20\text{ ng/cm}^2)=38$ ng/cm. The net flux of IAA is the product of the mass per unit length and the transport velocity.

The detailed boundary conditions on the simulation domain are described in Appendix 2. Of particular interest here are the sources and sinks of IAA. (1) There is a uniform source of IAA along the top edge of the domain, representing a net flux Φ_1 from the main branch. (2) There is a second source of IAA that enters the domain along the circular boundary, representing a net flux Φ_2 from the lateral branch. (3) There is a sink of IAA along the bottom edge of the square domain. The sink does not have a preset magnitude. Rather, all IAA that reaches the bottom edge is removed. This represents the continued basipetal transport of IAA from the junction into the subjacent branch.

To simplify our discussion, we set the model parameters and the input fluxes to be constant and seek solutions for the grain pattern that are time-independent. The true conditions in the cambium are known to be more variable (see e.g., Sundberg et al. 1993; Uggla et al. 1996; Funada et al. 2001; Powers et al. 2003), but our modeling results are intended to be illustrative rather than conclusive. Kramer (2002) surveys the relevant literature and takes v=10 mm/h, $D_{\parallel}$=5.0 mm^2/h, and $D_{\perp}$=1.2 mm^2/h as reasonable values for the parameters characterizing IAA transport. We continue to use these values here.

In Appendix 1 we show that time-independent grain patterns depend on K and μ only through the dimensionless parameter $\lambda = Kv/(\mu D_{\parallel} m_1)$, where m_1 is the mass of IAA per unit area at the top of the domain. It characterizes the relative strength of the cellular interactions that tends to keep the grain straight (K) and the chemotactic orientation of fusiform cells in response to IAA gradients (μ). A larger λ signals a "stiff" grain pattern in which grain line curvature is disfavored. We therefore refer to λ as the grain stiffness.

A comment on the display of grain patterns: it is common practice to visualize wood grain using *grain lines* (Phillips et al. 1981; Andre 2000; Foley 2001). We use the same technique to display the cambial grain pattern. To construct a grain line: (1) start at an arbitrary point in the cambium, (2) take a small step in the direction of the grain, (3) find the grain direction at the new location, and (4) take another step. This process, repeatedly applied, will draw a curve whose tangent is everywhere parallel to the grain direction. Note that the starting point of a grain line is arbitrary and does not necessarily correspond to any specific anatomical feature in the xylem.

Results and discussion

Our simulations cover a range of IAA flux ratios, Φ_2/Φ_1=0–0.72, and a range of grain stiffness λ=0.1–10. The value λ=0.1 is approximately correct for cottonwood (*Populus deltoides*), as determined by a comparison of wood grain patterns to simulation results (Kramer and Groves 2003). Informal observation of wood grain patterns in other temperate tree species suggests that cottonwood has a relatively low value of λ. Thus, 0.1–10 is likely to be a good representative range.

Figures 5, 6 and 7 show model results for the grain patterns at λ=0.1, 1, and 10, respectively. In each case, an increase in Φ_2/Φ_1 yields an increase in the amount of grain captured by the lateral branch. For $\lambda\leq1$, the relationship is especially simple—the fraction of the circumference of the

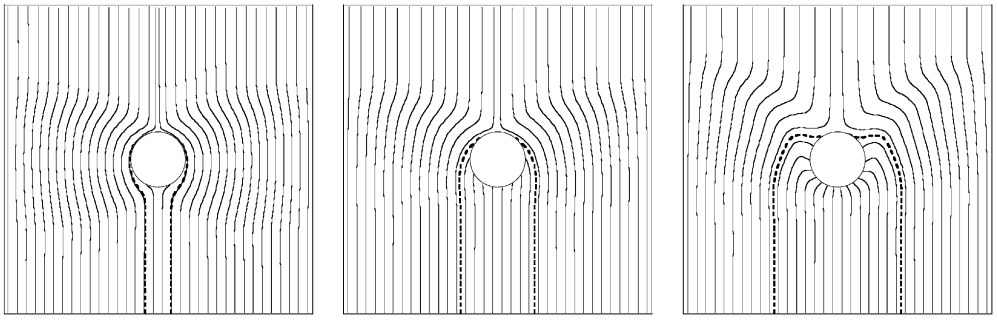

Fig. 5 Model results for the wood grain pattern at a junction between two live branches, grain stiffness parameter λ=0.1. The flux of IAA into the junction from the lateral increases from left to right, Φ_2/Φ_1=0.11, 0.33, 0.72. *Dashed lines* indicate the boundary of the grain captured by the lateral branch. Other parameters: v=10 mm/h, $D_{\parallel}$=5.0 mm^2/h, and $D_{\perp}$=1.2 mm^2/h. Size of square cambial domain, 34×34 mm^2. Radius of circular branch insertion, 3.0 mm

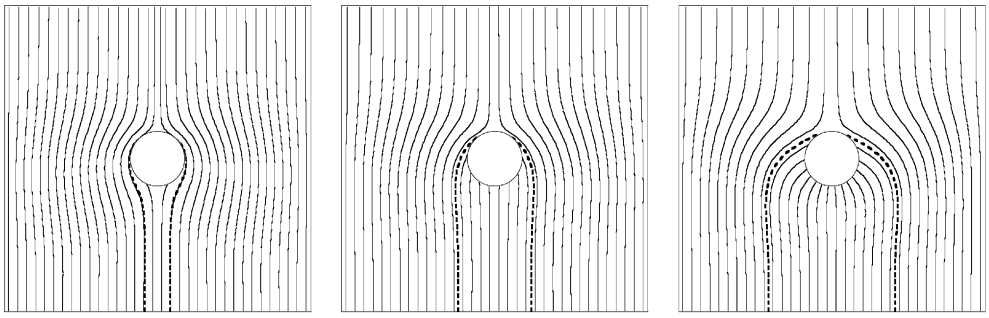

Fig. 6 Model results for the wood grain pattern at a junction between two live branches, grain stiffness parameter λ=1. The flux of IAA into the junction from the lateral increases from left to right, Φ_2/Φ_1=0.11, 0.33, 0.72

subjacent stem captured by the lateral is equal to ratio of the fluxes.

The effect of varying λ on the grain pattern is more subtle. Note the appearance of pronounced bends in the grain above the lateral branch in Fig. 5. In Figs. 6 and 7 the bends are progressively smoothed out, in accord with our description of λ as an effective grain line stiffness.

Figures 8 and 9 show model results for the case of a dead lateral branch. The grain patterns continue the trends visible in Figs. 5, 6 and 7. As expected, the dead lateral captures negligible grain for $\lambda \leq 1$. Surprisingly, the dead lateral does capture some grain for λ=10. Note also the significant accumulation of IAA above the lateral and the depletion below. For λ=10, the gradients of IAA near the lateral branch are not enough to deflect the grain lines around the curve of the circular branch insertion. It may be that λ=10 is an unrealistically large value for the grain stiffness.

Our results suggest that the export of IAA out of a branch is the means by which it captures grain from the subjacent stem. If IAA export stops, the grain reorients to circumvent the branch. Note the importance of the flux ratio in the preceding discussion—grain capture will increase under increased IAA export from the lateral, and also under decreased flux through the main branch or stem. Subject to the caveats about hydraulic conductivity discussed at the bottom of this section, an increase in grain capture will allow the branch increased access to the water resources of the stem. The flux of IAA in the main stem thus emerges as a possibly important variable for the regulation of lateral branch vigor. Note that this proposed regulatory mechanism acts at the branch junction and does not require IAA from the main stem to undergo acropetal transport into the lateral itself.

The assumption of branch autonomy says that the relative vigor of a branch is set by its morphology and its light environment (Sprugel et al. 1991). Our modeling suggests that a third variable contributing to the vigor of a branch is the net flux of IAA through the stem to which it is attached. This should be considered as one possible explanation for the growing list of known violations of branch autonomy (see Introduction). For example, consider Sprugel's observation that otherwise similar branches will be more vigorous if they are attached to a stressed crown as compared to an unstressed crown ("Milton's Law") (Sprugel 2002). He cites evidence for this effect in silver fir (*Abies amabilis*), Scots pine (*Pinus sylvestris*), *Litsea acuminata*, mountain birch (*Betula pubescens*), and Douglas fir (*Pseudotsuga menziesii*). Auxin-mediated grain capture could account for this if, in the species under consideration, less vigorous crowns tend to synthesize and/or export smaller amounts of IAA to the stem. Laterals would thus be better able to compete for the water resources of the tree.

We know of few published studies that allow us to test whether the stem of a stressed tree has a lower flux of IAA. An accurate comparison would require simultaneous measurement of the IAA distribution, transport speed, and the radius of the cambial cylinder. As far as we know, this has not been done. However, available studies indicate that stressed trees have smaller amounts of IAA, expressed per unit cambial area or per unit stem length. Funada et al. (1987, 2001) examined the stems of red pine (*Pinus densiflora*) trees that had been pruned to 20, 40, or 60% of their pre-existing crown size. The stems of trees that had been pruned more heavily contained smaller amounts of IAA on average. Uggla et al. (1998) reported the amount of IAA and the diameter of stems in fast-growing and slow-growing specimens of Scots pine (*Pinus sylvestris*).

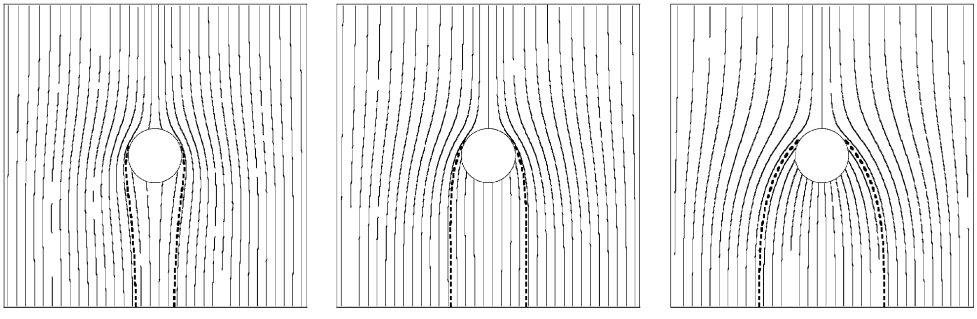

Fig. 7 Model results for the wood grain pattern at a junction between two live branches, grain stiffness parameter λ=10. The flux of IAA into the junction from the lateral increases from left to right, Φ_2/Φ_1=0.11, 0.33, 0.72

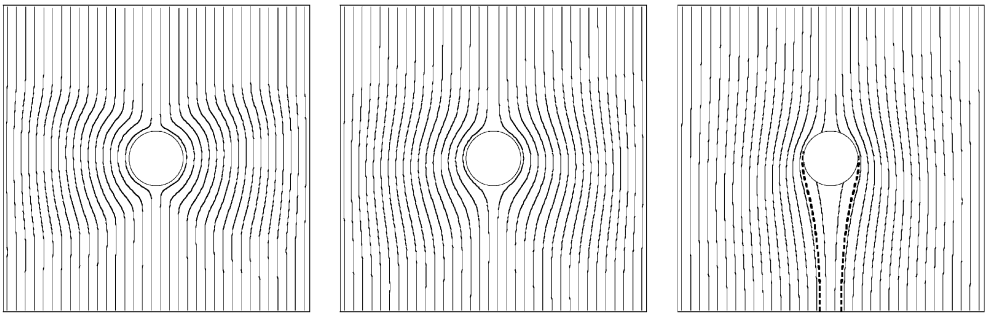

Fig. 8 Model results for the wood grain pattern at a branch junction where the lateral is dead, $\Phi_2/\Phi_1=0$. The grain stiffness parameter increases from left to right, $\lambda=0.1$, 1, 10. Other parameters same as Fig. 5

The fast-growing specimens (growing in a thinned and fertilized plot) had a mass of IAA per unit cambial area that was about twice as high compared to the slow-growing specimens. Expressed as mass per unit stem length, the difference was even more pronounced. The data for Scots pine thus favor a possible role for auxin-mediated grain capture in Milton's Law.

IAA's role in grain capture might also provide a plausible explanation for the phenomenon of apical control. If the flux of IAA in the stem increases from crown to base, then laterals lower in the crown will have greater difficulty in capturing grain from the stem. In this way, laterals closer to the ground may be deprived of sufficient water for growth despite their proximity to the roots.

To consider this possibility, we return to the published data on Scots pine (Uggla et al. 1998). All six specimens analyzed by Uggla et al. (1998) show an increase in the mass of IAA per unit length as measured between the crown interior (9th internode) and the crown base, with a mean increase of 30%. However, expressed as mass per unit area, the amount of IAA stays roughly the same or decreases over the same distance, with a mean decrease of 18%. The case for auxin-mediated grain capture as a mechanism for apical control in Scots pine is thus equivocal.

The theory of Aloni and Zimmermann (1983) provides additional but circumstantial evidence that the auxin concentration does not increase basipetally along the stem. They argue that the diameter and number density of newly-formed vessels in hardwood stems are determined by the concentration of IAA in the cambium. In this view, the typical basipetal increase (decrease) in the diameter (density) of vessels is an indication that the auxin concentration decreases from tree apex to base. While this does not rule out a role for IAA flux in the establishment of apical control, it certainly recommends some caution in the application of our results to ideas about tree form.

Further experimental work is needed to determine the significance of grain capture to the hydraulic architecture of trees and the vigor of branches. First, it needs to be verified that IAA flux from a lateral branch can affect grain patterns in the way suggested. As far as we know, there are neither published data on the flux of IAA through lateral branches in any species, nor are there many data on the relationship between the vigor of a tree and the distribution of IAA in the stem (excepting those papers cited above). Both require systematic study.

Even if the proposed mechanism of grain capture is largely correct, it should be remembered that hydraulic conductivity depends on many features of xylem anatomy (Tyree and Ewers 1991; Aloni et al. 1997). Most important is the diameter of the water conducting elements—vessels in hardwoods and tracheids in softwoods—since conductivity increases with the fourth power of diameter. Other factors affecting net conductivity include the length of the conducting elements, the width of the current year's annual ring, and the total number of annual rings that participate in transport. Conclusive work should consider all these factors.

One more caveat is that the cambial grain pattern is not unchanging over time. Thus, the degree to which the cambial grain pattern is an indication of the net water transport through the xylem depends on the number of annual rings that participate in the transport and the grain's rate of change (Kozlowski and Winget 1963; Zimmermann and Brown 1971; Ellmore and Ewers 1986). In ring-porous hardwood species, flow is typically concentrated in the large vessels of the outermost annual ring. In diffuse-

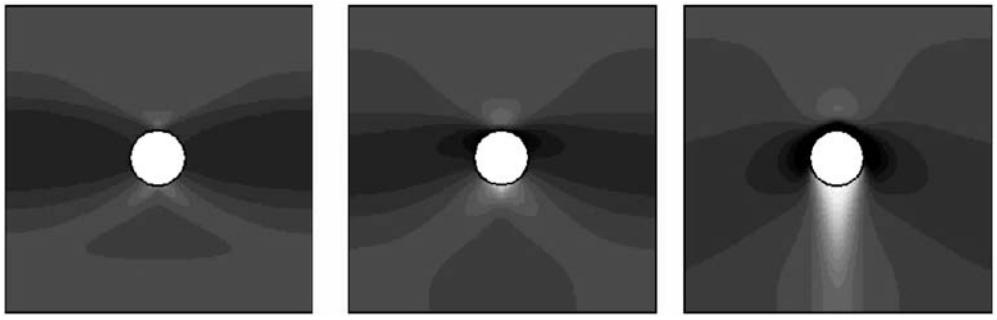

Fig. 9 Model results for the distribution of IAA corresponding to the grain patterns shown in Fig. 8. *Darker grays* correspond to higher concentrations. The IAA source at the top of the image is 20.0 (ng IAA)/cm^2. Each step in *grayscale* represents an increase of 1.4 (ng IAA)/cm^2. For $\lambda=10$, note the accumulation of IAA above the branch and the depletion below

porous hardwoods and softwoods, on the other hand, flow typically occurs through several annual rings. It is also possible that the grain at a branch junction may undergo dramatic swings during one growing season, as suggested by Shigo (1985). While we believe Shigo overstates the case, the possibility of seasonal grain changes needs to be evaluated when considering the relationship between grain and hydraulic architecture.

To conclude, we would like to speculate further about the role of IAA in the tree. The IAA undergoing basipetal transport through a branch is synthesized mainly in the most distal parts of the tree - growing leaves and buds (Sundberg and Uggla 1998; Aloni et al. 2003). Vigorous branches, which by definition have more growing tissues, are thus expected to have a higher flux of IAA than stressed branches. In this way, IAA export from a branch serves as an indicator for the water needs of more distal tissues. The grain capture mechanism appears to be a straightforward way for the tree to decide, based on need and the potential for future growth, how the water resources of the stem should be divided among branches.

Acknowledgements We are grateful to Simon's Rock College for the support of this research through the provision of a Faculty Development Fund and student research internships.

Appendix 1. Model equations

In this appendix we discuss the differential equations used in our model of wood grain at a branch junction. We begin with Eqs. 1 and 2 from Kramer and Groves (2003) and use their notation. The model is a pair of coupled, nonlinear partial differential equations in the variables m and $\mathbf{u}$, where m is the local mass of IAA per unit area of cambial surface and $\mathbf{u}$ is the local grain direction. The equations as cited have been transformed to the dimensionless variables $r' = rv/D_{\|}$, $t' = tK(v/D_{\|})^2$, and $m' = m/\langle m \rangle$, where $\langle m \rangle$ is a characteristic IAA concentration (we use the value $m=m_1$ imposed at the top of the simulation domain). Since we are seeking time-independent solutions, we set $\partial m/\partial t=0$ and $\partial \mathbf{u}/\partial t=0$. Dropping all primes gives:

$$\nabla \cdot \left[(\nabla_{\|} m - m)\hat{u} + (r_D \nabla_{\perp} m)\hat{w} \right] = 0 \tag{1}$$

$$\nabla^2 u + 2L^2 u(1-u^2) + 1\lambda\left[-(\nabla m)\left(3 - u^2 2\right) + (u \cdot \nabla m)u \right] = 0 \tag{2}$$

Following Kramer and Groves (2003), we set $r_D=0.23$ and $L=0.5$ for all the simulations reported in this paper. This leaves just one dimensionless parameter of interest, $\lambda = Kv/(\mu D_{\|} m_1)$.

Appendix 2. Boundary conditions

Separate from the model equations that dictate the solution in the interior of the simulation domain (see Appendix 1), one also needs to specify the shape of the domain and the boundary conditions on m and $\mathbf{u}$. As shown in Fig. 4, we use a square simulation domain of side S, with an disk of radius R excised from the center.

Fluxes There is a uniform flux of IAA into the domain at the top edge of the square and a second flux into the domain at the edge of the disk. These two fluxes represent the IAA supplied by the two distal branches. There is an IAA sink along the bottom edge that allows IAA to drain out of the domain via active transport. Side-to-side the domain has periodic boundary conditions, which is to say that IAA exiting the domain along the right edge immediately re-enters on the left and vice versa. This is not a necessity, but it is a useful means to enforce IAA conservation.

To set the apical flux, we impose the conditions $m=m_1$ and $\partial m/\partial y=0$. The net flux into the domain through the top edge is thus $\Phi_1=m_1 vS$. Implementing the flux at the circular boundary was nontrivial. Rather than imposing a condition at the boundary per se, we include the disk as part of the simulation domain. At each time step, every lattice site in the disk is given a small additional mass of IAA, Δm. The direction of active transport at all lattice sites in the disk is chosen to be radially outward, so that all mass deposited in the disk eventually exits the disk. The value of Δm is chosen so the net flux out of the disk is Φ_2.

Grain The grain direction along the top and side edges of the square domain is chosen to point downward ($\mathbf{u}=-\mathbf{e}_y$). We impose the Neumann condition $\partial \mathbf{u}/\partial y=0$ at the bottom edge. The condition on $\mathbf{u}$ at the boundary of the disk is again problematic. Since we want the flux of IAA to point radially outward, we originally chose $\mathbf{u}=\mathbf{e}_r$ on the disk boundary. While this works fine for $\lambda<1$, it causes problems when the grain stiffness is too large. In particular, it leads to an anomalously large region of approximately radial grain outside the disk. The fix for this problem was to recognize that the direction of IAA active transport in the disk could be uncoupled from the value for $\mathbf{u}$ as it appears in the calculation of the Laplacian (see Eq. 2, Appendix 1). We then set $\mathbf{u}=0$ at the boundary of the disk.

References

Aloni R, Alexander JD, Tyree MT (1997) Natural and experimentally altered hydraulic architecture of branch junctions in *Acer saccharum* Marsh. and *Quercus velutina* Lam. trees. Trees 11:255–264

Aloni R, Schwalm K, Langhans M, Ullrich C (2003) Gradual shifts in sites of free-auxin production during leaf-primordium development and their role in vascular differentiation and leaf morphogenesis in Arabidopsis. Planta 216:841–853

Aloni R, Zimmermann MH (1983) The control of vessel size and density along the plant axis: a new hypothesis. Differentiation 24:203–208

Andre JP (2000) Heterogeneous, branched, zigzag and circular vessels: unexpected but frequent forms of tracheary element files: description—localization—formation. In: Savidge RA, Barnett J, Napier R (eds) Cell and molecular biology of wood formation. BIOS Scientific, Oxford, pp 284–293

Becker P, Meinzer FC, Wullschleger SD (2000) Hydraulic limitation of tree height: a critique. Funct Ecol 14:4–11

Brooks J, Schulte P, Bond B, Coulombe R, Domec J-C, Hinckley TM, McDowell N, Phillips N (2002) Does foliage on the same branch compete for the same water? Experiments on Douglas-fir trees. Trees 17:101–108

Brown C, McAlpine R, Kormanik P (1967) Apical dominance and form in woody plants: a reappraisal. Am J Bot 54:153–162

Catesson AM (1990) Cambial cytology and biochemistry. In: Iqbal M (ed) The vascular cambium. Wiley, New York

Cline MG (1997) Concepts and terminology of apical dominance. Am J Bot 84:1064–1069

Eisner N, Gilman E, Grabosky J (2002a) Branch morphology impacts compartmentalization of pruning wounds. J Arboric 28:99–105

Eisner N, Gilman E, Grabosky J, Beeson R (2002b) Branch junction characteristics affect hydraulic segmentation in red maple. J Arboric 28:245–251

Ellmore GS, Ewers FW (1986) Fluid flow in the outermost xylem increment of a ring-porous tree, *Ulmus americana*. Am J Bot 73:1771–1774

Foley C (2001) A three-dimensional paradigm of fiber orientation in timber. Wood Sci Technol 35:453–465

Funada R, Sugiyama T, Kubo T, Fushitani M (1987) Determination of indole-3-acetic acid levels in *Pinus densiflora* using the isotope dilution method. Mokuzai Gakkaishi 33:83–87

Funada R, Mizukami E, Kubo T, Fushitani M, Sugiyama T (1990) Distribution of indole-3-acetic acid and compression wood formation in the stems of inclined *Cryptomeria japonica*. Holzforschung 44:331–334

Funada R, Kubo T, Sugiyama T, Fushitani M (2002) Changes in levels of endogenous plant hormones in cambial regions of stems of Larix kaempferi at the onset of cambial activity in springtime. J Wood Sci 48:75–80

Funada R, Kubo T, Tabuchi M, Sugiyama T, Fushitani M (2001) Seasonal variations in endogenous indole-3-acetic acid and abscisic acid in the cambial region of *Pinus densiflora* Sieb. et Zucc. stems in relation to earlywood-latewood transition and cessation of tracheid production. Holzforschung 55:128–134

Goulet J, Messier C, Nikinmaa E (2000) Effect of branch position and light availability on shoot growth of understory sugar maple and yellow birch saplings. Can J Bot 78:1077–1085

Green DW, Winandy JE, Kretschmann DE (1999) Mechanical properties of wood handbook: wood as an engineering material. Forest products laboratory, USDA Forest Service, Madison, Wis.

Harris JM (1969) On the causes of spiral grain in corewood of radiata pine. N Z J Bot 7:189–213

Harris JM (1989) Spiral grain and wave phenomena in wood formation. Springer, Berlin Heidelberg New York

Henriksson J (2001) Differential shading of branches or whole trees: survival, growth, and reproduction. Oecologia 126:482–486

Iqbal M, Ghouse AKM (1990) Cambial concept and organization. In: Iqbal M (ed) The vascular cambium. Wiley, New York, pp 1–28

Kirschner H, Sachs T, Fahn A (1971) Secondary xylem reorientation as a special case of vascular tissue differentiation. Isr J Bot 20:184–198

Kozlowski TT, Winget CH (1963) Patterns of water movement in forest trees. Bot J 124:301–311

Kramer EM (2002) A mathematical model of pattern formation in the vascular cambium of trees. J Theor Biol 216:147–158

Kramer EM, Groves JV (2003) Defect coarsening in a biological system: the vascular cambium of cottonwood trees. Phys Rev E 67:041914

Larson PR (1994) The vascular cambium. Springer, Berlin Heidelberg New York

Lev-Yadun S, Aloni R (1990) Vascular differentiation in branch junctions of trees: circular patterns and functional significance. Trees 4:49–54

Mattheck C, Kubler H (1995) Wood: the internal optimization of trees. Springer, Berlin Heidelberg New York

Nikinmaa E, Messier C, Sievanen R, Pettunen J, Lehtonen M (2003) Shoot growth and crown development: effect of crown position in three-dimensional studies. Tree Physiol 23:129–136

Phillips GE, Bodig J, Goodman JR (1981) Flow-grain analogy. Wood Sci 14:55–64

Powers SJ, Brain P, Barlow PW (2003) First-order differential equation models with estimable parameters as functions of environmental variables and their application to a study of vascular development in young hybrid aspen stems. J Theor Biol 222:219–232

Rudinsky JA, Vite JP (1959) Certain ecological and phylogenetic aspects of the pattern of water conduction in conifers. For Sci 5:259–266

Ryan MG, Yoder BJ (1997) Hydraulic limits to tree height and tree growth. Bioscience 47:235–242

Savidge RA (1996) Xylogenesis, genetic and environmental regulation. IAWA J 17:269–310

Schulte P, Brooks J (2003) Branch junctions and the flow of water through xylem in Douglas-fir and ponderosa pine stems. J Exp Bot 54:1597–1605

Shigo AL (1985) How tree branches are attached to trunks. Can J Bot 63:1391–1401

Shigo AL (1991) Modern arboriculture. Shigo and Trees Association, Durham, N.H.

Sperry JS, Hacke UG, Oren R, Comstock JP (2002) Water deficits and hydraulic limits to leaf water supply. Plant Cell Environ 25:251–263

Sprugel DG (2002) When branch autonomy fails: Milton's Law of resource availability and allocation. Tree Physiol 22:1119–1124

Sprugel DG, Hinckley TM, Schapp W (1991) The theory and practice of branch autonomy. Annu Rev Ecol Syst 22:309–334

Stoll P, Schmid B (1998) Plant foraging and dynamic competition between branches of *Pinus sylvestris* in contrasting light environments. J Ecol 86:934–945

Sundberg B, Ericsson A, Little CHA, Nasholm T, Gref R (1993) The relationship between crown size and ring width in *Pinus sylvestris* L. stems: dependence on indole-3-acetic acid, carbohydrates, and nitrogen in the cambial region. Tree Physiol 12:347–362

Sundberg B, Uggla C (1998) Origin and dynamics of indoleacetic acid under polar transport in Pinus sylvestris. Physiol Plant 104:22–29

Sundberg B, Uggla C, Tuominen H (2000) Cambial growth and auxin gradients. In: Savidge RA, Barnett J, Napier R (eds) Cell and molecular biology of wood formation. BIOS Scientific, Oxford, pp 169–188

Takenaka A (2000) Shoot growth responses to light microenvironment and correlative inhibition in tree seedlings under a forest canopy. Tree Physiol 20:987–991

Tuominen H, Peuch L, Fink S, Sundberg B (1997) A radial concentration gradient of indole-3-acetic acid is related to secondary xylem development in *Populus*. Plant Physiol 115:577–585

Tuominen H, Puech L, Regan S, Fink S, Olsson O, Sundberg B (2000) Cambial region specific expression of the *Agrobacterium iaa* genes in transgenic aspen visualized by a linked *uidA* reporter gene. Plant Physiol 123:531–541

Tyree MT, Alexander JD (1993) Hydraulic conductivity of branch junctions in three temperate tree species. Trees 7:156–159

Tyree MT, Ewers FW (1991) The hydraulic architecture of trees and other woody plants. New Phytol 119:345–360

Uggla C, Moritz T, Sandberg G, Sundberg B (1996) Auxin as a positional signal in pattern formation in plants. Proc Natl Acad Sci USA 93:9282–9286

Uggla C, Mellerowicz E, Sundberg B (1998) Indole-3-acetic acid controls cambial growth in Scots pine by positional signalling. Plant Physiol 117:113–121

Zagorska-Marek B, Little CHA (1986) Control of fusiform initial orientation in the vascular cambium of Abies balsamea stems by indole-3-ylacetic acid. Can J Bot 64:1120–1128

Zimmermann MH, Brown C (1971) Trees: structure and function. Springer, Berlin Heidelberg New York